DOI: 10.3901/CJME.2012.03.***, available online at www.springerlink.com; www.cjmenet.com; www.cjmenet.com.cn

Novel 6-DOF Wearable ... with Pneumatic Force-Feedback for Bilateral Teleoperation

ZHANG Jiafan[1,2,*], FU Hailun[2], DONG Yiming[1], ZHANG Yu[1], YANG Canjun[1], and CHEN Ying[1]

1 *State Key Laboratory of Fluid Power Transmission and Control, Zhejiang University,Hangzhou 310027, China*
2 *Zhejiang Province Instituteof Metrology,Hangzhou 310027, China*
3 *National Die & Mold CAD Engineering Research Center, Shanghai Jiao Tong Univers*

Received September 8, 2011; revised January 18, 2012; accepted February 23, 2012

Abstract: Magnetic drive pump has gotten great achievement and has bee... fields. Currently, the researches on magnetic drive pump have focused on hydraulic design, bearing, axial ... netic drive pump with low flow and high head have been developed overseas. However, low efficiency and large size are the common disadvantages for the magnetic drive pump. In order to study the performance of high-speed magnetic drive pump, FLUENT is used to simulate the inner flow field of magnetic drive pumps with different rotate speeds, and get velocity and pressure distributions of inner flow field. According to analysis the changes of velocity and pressure to ensure the stable operation of pump and avoid cavitation. Based on the analysis of velocity and pressure, this paper presents the pump efficiency of magnetic drive pumps with different rotated speeds by calculating the power loss in impeller and volute, hydraulic loss, volumetric loss, mechanical loss and discussing the different reasons of power loss between the magnetic drive pumps with different rotated speeds. In addition, the magnetic drive pumps are tested in a closed testing system. Pressure sensors are set in inlet and outlet of magnetic drive pumps to get the p... got by calculating the power loss between the input power and the outlet power. The results of simulation and test are s... which shows that the method of simulation is feasible. The proposed research provides the instruction to design high-speed magnetic drive pump.

Key words: exoskeleton arm, teleoperation, pneumatic force-feedback, hybrid fuzzy control

1 Introduction

At first look at modern society, more and more robots and automated devices are coming into our life and serve for human. But on even further i... mechatronic devices replace h... lower levels, essentially provi... routine tasks. Human control is... levels just as the term human ... which is coined by SH... master-slave teleoperation syst... of radioactive materials in a c... GOERTZ, et al[2], was the typi... Hereafter, exoskeleton arms with force-feedback have... widely developed in the fields of robot teleoperatio... haptic interface to enhance the performance of the h... operator, also in the exciting applications in surgery planning, personnel training, and physical rehabilitation. DUBEY, et al[3], developed a methodology to incorporate sensor and r... ance into human controlled teleoperation systems. In their approach, the human operator was retained at all phases of the operation, and was assisted by adjusting system parameters which were not under direct control by the operator, specifically, ...ping of positions and velocities between the master ...e and their impedance parameters. The ESA human ...skele- ton was developed to enable force-feedback ...ipulation on the exterior of the international space ...botic arms[4]. In recent work[5–6], ... has been used to control the ...y new concepts were applied in ...everal researchers from Korea ... Technology (KIST) introduced ...o the exoskeleton and designed a ...e 3RPS parallel mechanism[11–12]. They explored a new exoskeleton-type master arm, in which the electric brakes with the torque sensor beams were used for force reflection[14]. Likewise, the authors gave out a 2-port network model to describe the bilateral remote manipulation in the view of the control theory [15–17].

In this research, a wearable exoskeleton arm, ZJUESA, ... man-machine system is designed and a ...lly distributed teleoperation control system is ... includes three main levels: ①

* Corresponding author. E-mail: caffeezhang@hotmail.com
This project is supported by National Natural Science Foundation of China (Grant No. 50305035), National Hi-tech R... Program of China(863 Program, Grant No. ##), ... Science Foundation of China((Grant No. ##), and ... Natural Science Foundation of China((Grant No. ##)

supervisor giving the command through the exoskeleton arm in safe zone with the [illegible] interface; ② slav[illegible]; ③ data trans[illegible] master-slave through the Internet or Ethernet. In section 2, by using the orthogonal experiment design method, the design foundation of ZJUESA and its optimal design are presented. Then in section 3, we describe a novel hybrid fuzzy control system for the force feedback on ZJUESA. Consequently, the force feedback control simulations and experiment results analysis are presented in section 4, followed by discussions and conclusions.

Even header Font Size 8 p, Line Spacing single, Paragraph Spacing After 1.2 p

2 Configuration of the Exoskeleton Arm System

The master-slave control is widely employed in the robot manipula[illegible]r the keyboard is the routi[illegible]ster-slave control system. [illegible] paper is shown in Fig. 1.

A paragraph is followed by a blank line, when figures follow it.

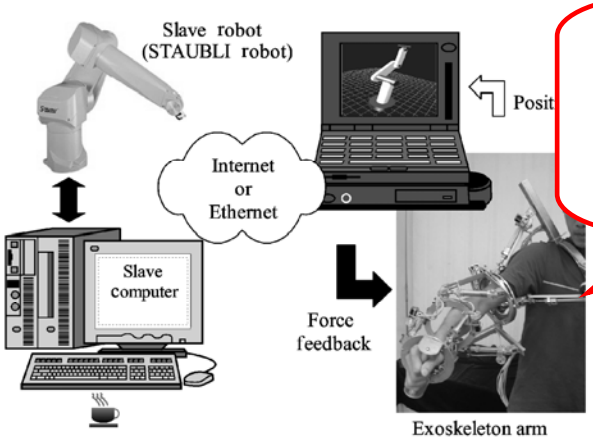

Fig. 1. Configuration of the exoskeleton arm system

Requirements of figure and table:

Image	resolution
Grayscale	< 150 | > 225
Color	< 150 | > 225
Bitmap	< 600 | > 900

Figure title Font Size 9 p, Line Spacing exactly 11 p, Paragraph Spacing Before 0.3 p; Leave one blank line after the figure title. figure text Font Size 7.5 p

In the syste[illegible] the joystick as[illegible] structure mecha[illegible] and can transfer the motions of human upper arm to the slave manipulator position-control-commands through the Internet or Ethernet between the master and slave computers. With this information, the slave manipulator mimics the motion of the operator. At the same time, the force-feedback signals, detected by the 6-axis force/torque sensor on the slave robot arm end effector, are sent back to indicate the pneumatic actuators for the force-feedback on ZJUESA to realize the bilateral teleoperation.

Since ZJUESA is designed by following the physiological parameters of the human upper-limb, with such a device the human operator can control the manipulator more comfortably and intuitively than the system with the joystick or the keyboard input.

3 Design of the Exoskeleton Arm

What we desire is an arm exoskeleton which is capable of following motions of the human upper-limb accurately and supplying the human upper-limb with proper force feedback if needed. In order to achieve an ideal controlling performance, we have to examine the structure of the human upper-limb.

Heading level two Font Size 10 p

3.1 Anatomy of human upper-limb

3.1.1 Upper-limb

Heading level three Font Size 10 p, italic, Paragraph Spacing Before 0.5 line

Recently, various [illegible] of the human upper-limb anatomy have [illegible]s of the arm that sta[illegible]ding muscles, tendons and bones are too complex to be utilized in mechanical design of an anthropomorphic robot arm. From the view of the mechanism, we should set up a more practicable model for easy and effective realization.

Fig. 2 introduces the configuration of human upper-limb and its equivalent mechanical model, which is a 7-DOF structure, including 3 degrees of freedom for shoulder (flexion/extension, abduction/adduction and rotation), 1 degree of freedom for elbow (flexion/extension) and 3 [illegible] extension, [illegible]ails about the [illegible]oints can be [illegible]e mechanical [illegible]onsidered as [illegible]n joint. It is a [illegible]ximate model for the human arm, and the base for the design and construction of exoskeleton arm-ZJUESA.

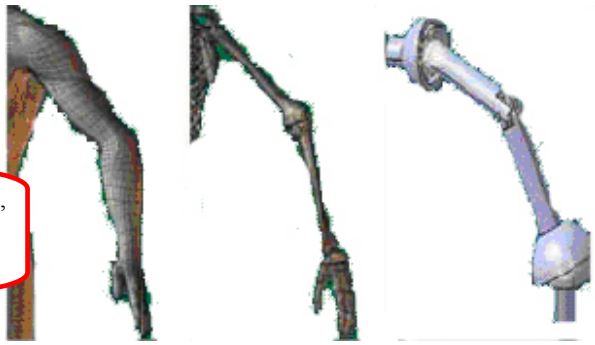

Fig. 2. Configuration of human upper limband its equivalent mechanical model

Leave two blank lines before a heading, when the heading follows a figure.

3.2 Mechanism of the exo[illegible]

Because the goal of this [illegible] of the human arm accurately for teleoperation, ZJUESA ought to make the best of motion scope of the human upper-limb and limit it as little as possible. A flexible structure with the same or similar configuration of human upper-limb is an ideal choice. Based on the anatomy of human upper-limb, the joint motion originates from extension or flexion of the muscle and ligament with each other to generate torque around the bones. Compared with the serial mechanism, the movements of the parallel mechanism are driven by the

prismatics, which act analogically to the human muscles and ligament. Besides, using th parallel mechanism not prismatics, which act ly to the human muscles lel mechanism not m lie on the surface of human upper-limb.

Odd header Font Size 10.5 p, Line Spacing single, Paragraph Spacing After 1.2 p

The 3RPS parallel mechanism is one of the simplest mechanisms. Fig. 3 explains the principle of the 3RPS parallel mechanism. KIM, et al[11], introduced it into the KIST design. Here we follow this concept. The two revolution degrees of freedom embodied in the 3RPS are for flexion/extension, abduction/adduction at shoulder. Its third translation degree of freedom along z axis can be used for the dimension adjustment of ZJUE operators. The prismatic joints are embod actuators, which are deployed to supply force reflective capability. Also displacement sensors are located along with the pneumatic actuators and the ring-shaped joints to measure their linear and angular displacements. At elbow, a crank-slide mechanism composed of a cylinder and links is utilized for flexion/extension. At wrist, since the abduction/adduction movement is so limited and can be indirectly reached by combination of the other j configuration by ignoring the effect shown in Fig. 4, the additional ring shoulder for the elbow rotation. Thus arm-ZJUESA has 6 degrees of freedom totally.

A paragraph is followed by one blank line, when a table follows it.

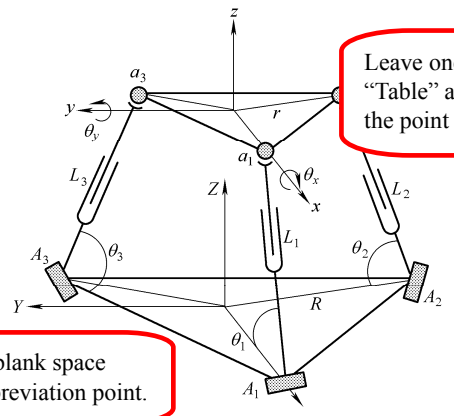

Leave one blank space after an abbreviation point.

Fig. 3. 3RPS parallel mechanism

Leave two blank spaces after the point of a figure number.

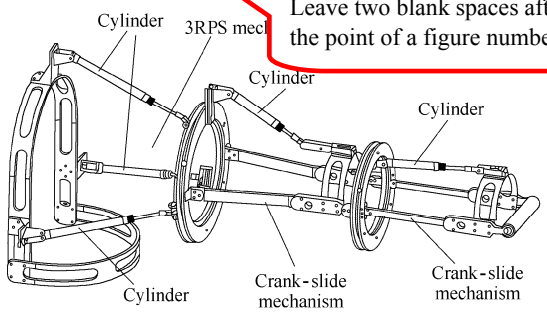

Fig. 4. Prototype of the exoskeleton arm-ZJUESA

3.3 Optimization design of ZJUESA

As nentioned above, the best design is to make the workspace of ZJUESA as fully cover the scope of the human upper-limb motion as possible. We employ the 3RPS parallel mechanism for the shoulder, whose workspace mainly influences the workspace of ZJUESA. The optimal design of 3RPS parallel mechanism for the shoulder is the key point of ZJUESA optimal design. However, it is a designing problem with multi-factors, saying the displacement of the prismatics (factor A), circumradius ratio of the upper and lower platforms (factor B), initial length of the prismatics (factor C), and their coupling parameters (factor $A*B$, $A*C$ and $B*C$) (Table 1) namely, its workspace, weight, size. So, ogonal experiment design method with key factors[21] and Eq. (1) gives the expression of the optimal target function of this problem:

A paragraph is followed by one blank line, when an equation follows it.

$$Q = F\left(L_0,\ \theta - \theta_x,\ \frac{r}{R}\right), \tag{1}$$

where L_0 is the initial length of the prismatics, R is the circumradius of the lower base in 3RPS mechanism, r is the circumradius of the upper base in 3RPS mechanism, θ is expected reachable angle ar reachable angle around axis.

Table title Font Size 9 p, bold, Paragraph Spacing After 0.3 line

Table 1. Factors and their levels mm

	A	B	C	$A*B$	$A*C$	$B*C$
	60	0.5	150	—	—	—
	80	0.438	160	—	—	—
	100	0.389	170	—	—	—
	—	—	18			

Leave one blank space after the word "Table" and two blank spaces after the point of a table number.

Table text Font Size 8 p, Line Spacing exactly 11 p; Leave one blank line after a table.

The orthogonal experiment d the ease with which levels c efficiency. The concept of orthogonal experiment design is discussed in Ref. [21] to obtain parameters optimization, finding the setting for each of a number of input parameters that optimizes the output(s) of the design. Orthogonal experiment design allows a decrease in the number of experiments performed with only slightly less accuracy than full factor testing. The orthogonal experiment design concept can be used for any complicated system being investigated, regardless of the nature of the system. During the optimization, all variables, even continuous ones, are thought of discrete "levels". In an orthogonal experiment design, the levels of each factors are allocated by using an orthogonal array[22]. By discretizing variables in this way, a design of experiments is advantageous in that it can reduce the number of combinations and is resistant to noise and conclusions valid over the entire region spanned by the control factors and their setting.

Table 2 describes an orthogonal experiment design array for 6 key factors[23]. In this array the first column implies the number of the experiments and factors A, B, C, $A*B$,

*A***B* and *B***C* are arbitrarily assigned to columns respectively. From Table 2, 36 trials of experiments are needed, with level of each factor for each trial-run indicated. The frame around a page number, Horizontal Position 1.8 cm Relative to a page represent the levels of each columns represent the experi sing that array. Each of the columns contains several assignments at each level for the corresponding factors. The levels of the latter three factors are dependent on those of the former three factors. The elements of the column IV, namely factor *A***B*, are determined by the elements in the columns I, II, and elements of column V, factor *A***C*, has the relationship with the elements of columns I, III, and the column VI, factor *B***C*, lies on the columns II, III.

Table 2. Orthogonal experiment design array L36 for 6 key factors

Experiment number	*A*	*B*	*C*	*A***B*	*A***C*	*B***C*	Result *Q*
1	1	1	1	1	1	1	Y_1
2	1	1	2	1	2	2	Y_2
3	1	1	3	1	3	3	Y_3
4	1	1	4	1	4	4	Y_4
5	1	2	1	2	1	5	Y_5
6	1	2	2	2	2	6	Y_6
⋮	⋮	⋮	⋮	⋮	⋮	⋮	⋮
33	3	3	1	9	9	9	Y_{33}
34	3	3	2	9	10	10	Y_{34}
35	3	3	3	9	11	11	Y_{35}
36	3	3	4	9	12	12	Y_{36}

The relation between column IV and columns I, II is that: if level of *A* is *n* and level of *B* is *m*, the level of *A***B* is 3(*n*–1)+*m*, where *n*=1, 2, 3 and *m*=1, 2, 3.

All the cases can be expressed as follows:

$$\begin{array}{lll}(1,1)\to 1 & (1,2)\to 2 & (1,3)\to 3;\\ (2,1)\to 4 & (2,2)\to 5 & (2,3)\to 6;\\ (3,1)\to 7 & (3,2)\to 8 & (3,3)\to 9.\end{array}$$

The first element in the bracket represents the corresponding level of factor *A* in Table 1 and the latter means the corresponding level of the factor *B*. Factor *A***B* has totally 9 levels, as factor *A* and factor *B* have 3 levels, respectively.

Likewise, the relation between column V and columns I, III is

$$\begin{array}{llll}(1,1)\to 1 & (1,2)\to 2 & (1,3)\to 3 & (1,4)\to 4;\\ (2,1)\to 5 & (2,2)\to 6 & (2,3)\to 7 & (2,4)\to 8;\\ (3,1)\to 9 & (3,2)\to 10 & (3,3)\to 11 & (3,4)\to 12.\end{array}$$

Also the relation between column VI and columns II, III is

$$\begin{array}{llll}(1,1)\to 1 & (1,2)\to 2 & (1,3)\to 3 & (1,4)\to 4;\\ (2,1)\to 5 & (2,2)\to 6 & (2,3)\to 7 & (2,4)\to 8;\\ (3,1)\to 9 & (3,2)\to 10 & (3,3)\to 11 & (3,4)\to 12.\end{array}$$

The optimal design is carried out according to the first three columns:

$$\begin{pmatrix} I_{A_1} \\ I_{A_2} \\ \vdots \\ I_{B*C_{11}} \\ I_{B*C_{12}} \end{pmatrix} = \begin{pmatrix} 1/9 & 1/9 & 1/9 & \cdots & 0 & 0 & 0 & 0 & 0 \\ 0 & 0 & 0 & \cdots & 0 & 0 & 0 & 0 & 0 \\ \vdots & \vdots & \vdots & & \vdots & \vdots & \vdots & \vdots & \vdots \\ 0 & 0 & 0 & \cdots & 0 & 0 & 0 & 1/3 & 0 \\ 0 & 0 & 0 & \cdots & 0 & 0 & 0 & 0 & 1/3 \end{pmatrix} \begin{pmatrix} Y_1 \\ Y_2 \\ \vdots \\ Y_{35} \\ Y_{36} \end{pmatrix}, \tag{2}$$

$$K_i = \max\{I_{ij}\} - \min\{I_{ij}\}, \tag{3}$$

where *i*= *A*, *B*, *C*, *A***B*, *A***C*, *B***C*; *j* is the number of *i* rank.

By Eqs. (2), (3) and the kinematics calculation of the 3RPS parallel m anism [35], the relationship between the target *Q* and d, as shown in Fig. 5. Leave one blank space after an abbreviation point.

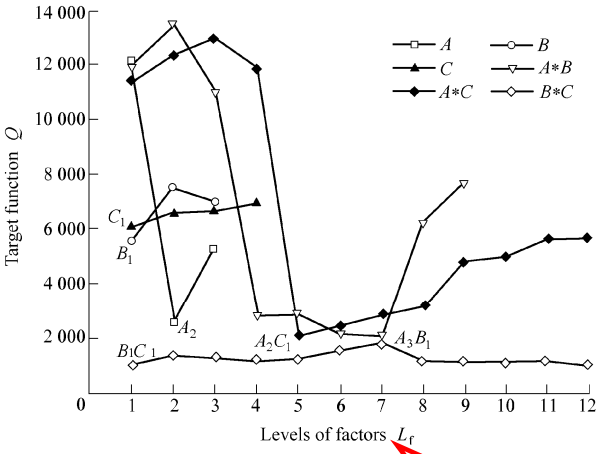

Fig. 5. Relation between levels of f

Leave two blank spaces between a variable's name and its symbol.

According to the plots in Fig. superiority and the degree of the infl each design factor. The factor with bigger extreme difference K_i, as expressed in Eq. (3) has more influence on *Q*. In this case, it can be concluded that the sensitivity of the factors *A***B* and *A***C* are high and factors *B***C* and *C* have weak influence, since K_{A*B} and K_{A*C} are much bigger than K_{B*C} and K_C. And the set A_3B_1, A_2C_1, A_2, B_1, C_1, B_1C_1 are the best combination of each factor levels. But there is a conflict with former 3 items in such a set. As their K_i have little differences between each other, the middle course is chosen. After compromising, we take the level 2 of factor *A*, the level 1 of factor *B* and the level 1 of factor *C*, namely *d* =80 mm, *r*/*R*=0.5, L_0=150 mm[32].

It is interesting to know how good the results derived from the above 36 trials are, when compared with all other possible combinations. Because of its mutual balance of orthogonal arrays, this performance ratio can be guaranteed by the theorem in non-parametric statistics[13]. It predicts

that this optimization is better than 97.29% of alternatives.

Combined with the kinematics and dynamics simulation of the 3RPS parallel mechanism and ZJUESA with chosen design parameters by ADAMS, we perform the optimal design. Table 3 indicates the joint range and joint torque of each joint on ZJUESA. It is apparent that ZJUESA can almost cover the workspace of human upper-limb well so that it can follow the motion of human operation upper-limb with little constrain, as shown in Fig. 6.

Table 3. Joint ranges and joint torques for each joint on ZJUESA

Joint on ZJUESA	Joint range θ/(°)	Joint torque T/(N • m)
Flexion/extension (shoulder)	–60–60	36
Abduction/adduction (shoulder)	–50–60	36
Rotation (shoulder)	–20–90	18
Flexion/extension (elbow)	0–90	28
Rotation (wrist)	–20–90	13
Flexion/extension (wrist)	0–60	28
Abduction/ adduction (wrist)	–	–

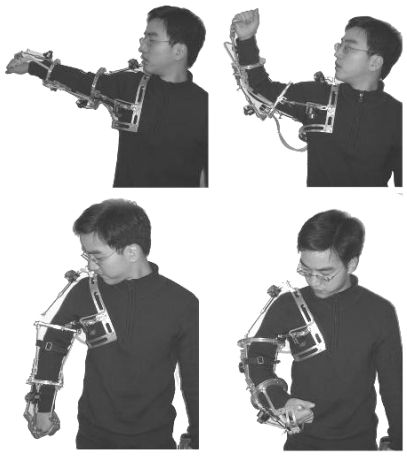

Fig. 6. Motion of exoskeleton arm following the operator

4 Hybrid Fuzzy-Controller for the Force Feedback On Zjuesa

In master-slave manipulation, besides the visual feedback and man-machine soft interface, the force feedback is another good choice to enhance the control performance. If the slave faithfully reproduces the master motions and the master accurately feels the slave forces, the operator can experience the same interaction with the teleoperated tasks, as would the slave. In this way the teleoperation becomes more intuitive.

In our bilateral teleoperation system with ZJUESA, a 6 axis force/torque sensor is mounted on the end effector of the slave manipulator and detects the force and torque acting on the end effector during performing the work. This information is transferred to the master site in real time. With dynamic calculation, the references of the generating force on actuators of ZJUESA are obtained. Hereafter, the feeling can be reproduced by means of the pneumatic system.

Eq. (4) expresses the relation between the force and torque on the end effector and the torques generating on the joints:

$$\boldsymbol{\tau} = \boldsymbol{J}^{\mathrm{T}} \boldsymbol{F} , \tag{4}$$

where $\boldsymbol{F}$—Force and torque on the

$\boldsymbol{F} = \begin{pmatrix} \boldsymbol{f} \\ \boldsymbol{n} \end{pmatrix}$,

$\boldsymbol{\tau}$—Torque on each joint,

$\boldsymbol{\tau} = (\tau_1 \quad \tau_2 \quad \cdots \quad \tau_6)^{\mathrm{T}}$,

$\boldsymbol{J}$—Jacobian matrix of ZJUESA.

Line Spacing single for the notes and other equations under an equation

By dividing the force arm, it is easy to get to the generating force on the joints, such as shoulder ring, elbow, wrist ring and wrist, as explained by Eq. (5):

$$\boldsymbol{f} = (f_4 \quad f_5 \quad f_6 \quad f_7)^{\mathrm{T}} = \left(\frac{\tau_3}{a_3} \quad \frac{\tau_4}{a_4} \quad \frac{\tau_5}{a_5} \quad \frac{\tau_6}{a_6} \right)^{\mathrm{T}} , \tag{5}$$

where a_i (i=3, 4, 5, 6) is the force arm of the shoulder ring, elbow, elbow ring and wrist joints, respectively.

As for the generating force of the prismatics on the 3RPS parallel mechanism, it can be calculated as follows[35]:

$$\begin{pmatrix} f_1 \\ f_2 \\ f_3 \end{pmatrix} = \boldsymbol{G}_F^f \begin{pmatrix} \boldsymbol{\tau}_{3\mathrm{RPS}} \\ \boldsymbol{f}_{3\mathrm{RPS}} \end{pmatrix} , \tag{6}$$

where $\boldsymbol{G}_F^f$—Jacobian matrix of 3RPS parallel mechanism,

$\boldsymbol{\tau}_{3\mathrm{RPS}}$—Torques on 3RPS parallel mechanism,

$\boldsymbol{\tau}_{3\mathrm{RPS}} = (\tau_1 \quad \tau_2)^{\mathrm{T}}$,

$\boldsymbol{f}_{3\mathrm{RPS}}$—Force on 3RPS parallel mechanism.

Therefore, with Eqs. (5), (6), the total seven force references are obtained for the pneumatic system on ZJUESA. Fig. 7 explains the scheme of the pneumatic cylinder-valve system for the force feedback.

Therefore, with Eqs. (5), (6), the total seven force references are obtained for the pneumatic system on ZJUESA. Fig. 7 explains the scheme of the pneumatic cylinder-valve system for the force feedback. Therefore, with Eqs. (5), (6), the total seven force references are obtained for the pneumatic system on ZJUESA. Fig. 7 explains the scheme of the pneumatic cylinder-valve system for the force feedback. Therefore, with Eqs. (5), (6), the total seven force references are obtained for the pneumatic system on ZJUESA. Fig. 7 explains the scheme of the pneumatic cylinder-valve system for the force feedback. Therefore, with Eqs. (5), (6), the total seven force references are obtained for the pneumatic system on ZJUESA. Fig. 7 explains the scheme of the pneumatic

cylinder-valve system for the force feedback. Therefore, with Eqs. (5), (6), the total seven force references are obtained for the pneumatic system on ZJUESA.

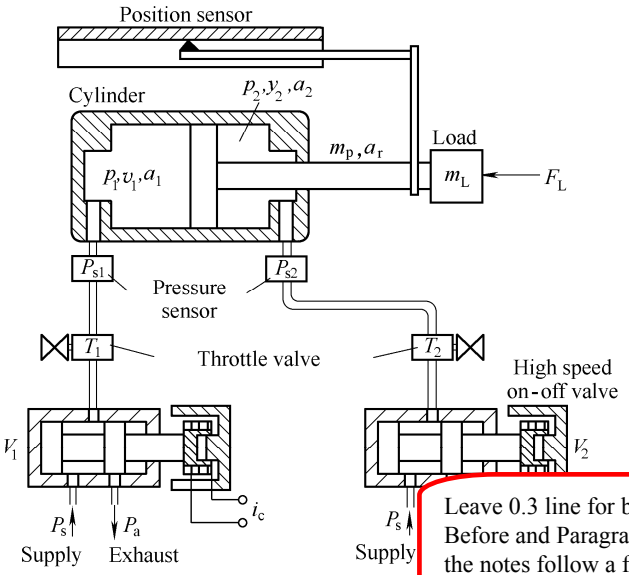

Leave 0.3 line for both Paragraph Spacing Before and Paragraph Spacing After, when the notes follow a figure title.

Fig. 7.　Scheme of the pneumatic cylinder-valve system

p_1, v_1, a_1—Pressure, volume and section area of cylinder chamber 1
p_2, v_2, a_2—Pressure, volume and section area of cylinder chamber 2
m_p—Mass of the piston
a_r—Section area of rod
m_L—Mass of load

Notes Font Size 8 p, Line Spacing single; Leave one blank line after the last line of the notes.

The high-speed on-off valves, as the actuating components in the system, are controlled by the pulse width modification (PWM) signals from the control units, respectively. Rather than the proportional or servo valve, this is an inexpensive and widely used method in the application of position and force control in the pneumatic system [23–28]. To simplify the control algorithm, there is just one valve on work at any moment. For instance, when a leftward force is wanted, the valve V_1 works and valve V_2 is out of work. Under this case, we can control the pressure p_1 in chamber 1 by modifying the PWM signals. Chamber 2 connects to the atmosphere at that time and the pressure p_2 inside the chamber 2 of cylinder is absolutely ambient pressure, and vice versa. At each port of the cylinder, there is a pressure sensor to detect the pressure value inside the chamber for the close-loop control. And the throttle valves are equipped for limiting the flow out of the chamber to reduce piston vibrations. In our previous work, we gave out the specific mathematic models of the system, including pneumatic cylinder, high-speed on-off valve and connecting tube[33].

However, the pneumatic system is not usually a well linear control system, because of the air compressibility and its effect on the flow line. Also the highly nonlinear flow brings troubles into the control. The conventional controllers are often developed via simple models of the plant behavior that satisfy the necessary assumptions, via the specially tuning of relatively simple linear or nonlinear controllers. As a result, for pressure or force control in such a nonlinear system, especially in which the chamber pressure vibrates rapidly, the conventional control method can hardly have a good performance.

Fortunately, the introduction of the hybrid control method mentioned, gives out a solution to this problem. But the traditional design of the hybrid controller is always complicated and only available to the proportion or servo valve system. In our system, we figured out a kind of novel hybrid fuzzy control strategy for the high-speed on-off valves, which is much simpler and can be realized by micro control units (MCUs) in the contributed architecture. This strategy is composed of two main parts: a fuzzy controller and a bang-bang controller. The fuzzy controller provides a formal methodology for representing, manipulating, and implementing a person's heuristic knowledge about how to control a system. It can be regarded as an artificial decision [illegible]s in a closed-loop system in real time and [illegible]n to get the control information either [illegible]sion maker who performs the control [illegible]dy, while the bang-bang controller is added to drive the response of the system much more quickly.

Fig. 8 shows the concept of the proposed hybrid fuzzy controller. The concept of multimode switching is applied to activate either the bang-bang controller or the fuzzy controller mode.

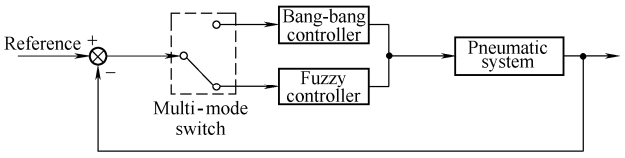

Fig. 8.　Concept of the hybrid fuzzy controller

Bang-bang control is applied when the actual output is far away from reference value. In this mode, fast tracking of the output is implemented. The fuzzy controller is activated when the output is near the set point, which needs accuracy control.

In the fuzzy-control mode, we use pressure error $e(t) = P_{\text{ref}}(t) - P_{\text{actual}}(t)$ and its change $\dot{e}(t)$ as the input variables on which to make decisions. On the other hand, the width of the high voltage in one PWM period is denoted as the output of the controller.

As mentioned above, the PC on master site works as the supervisor for real-time displaying, kinematics calculation and exchanges the control data with the slave computer and so on. For the sake of reducing the burden of the master PC, the distributed control system is introduced. Each control unit contains a Mega8 MCU of ATMEL Inc., working as a hybrid fuzzy-controller for each cylinder respectively, and forms a pressure closed-loop control. The controller samples the pressure in chamber with 20 kHz sampling rate by the in-built analog- digital converters. These controllers

keep in contact or get the differential pressure signals from the master PC through RS232, as depicted in Fig. 9. In this mode, fast tracking of the output is implemented.

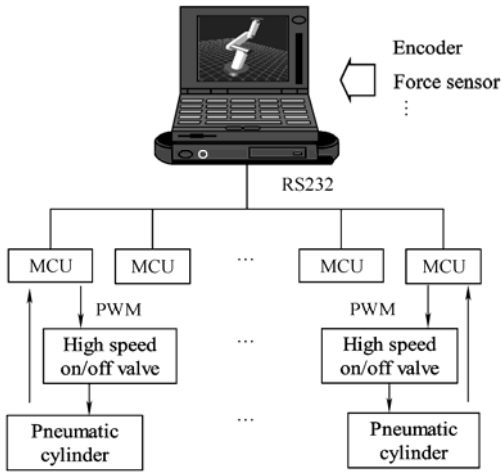

Fig. 9. Distributed control system of the master arm

5 Force Feedback Experiments

Fig. 10 gives out the set up of the force feedback experiments. The system includes the soft interface, data acquisition, Mega8 MCU experiment board, on-off valves, sensors of displacement and pressure, and the oscilloscope. We chose the cylinder DSNU-10-40-P produced by FESTO Inc. The soft signal generator and data acquisition are both designed in the LabVIEW, with which users may take advantage of its powerful graphical programming capability. Compared with other conventional programming environments, the most obvious difference is that LabVIEW is a graphical compiler that uses icons instead of lines of text. Additionally, LabVIEW has a large set of built-in mathematical functions and graphical data visualization and data input objects typically found in data acquisition and analysis applications.

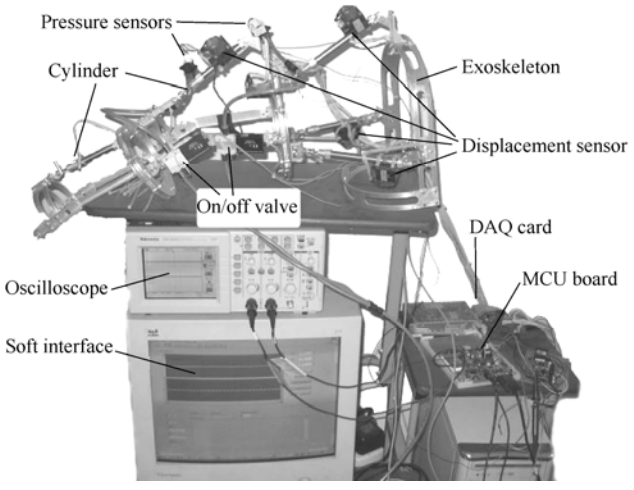

Fig. 10. Set-up of force feedback experiment

The plots in Fig. 11 give out experimental results of the chamber pressure outputs with step input signals on one joint. While at frequencies higher than 80 Hz, force is sensed through the operator's joint, muscle and tendon receptors, and the operator is unable to respond to, and low amplitude disturbances at these frequencies. We remove reflected force signals above 80 Hz band by fast Fourier transfer (FFT) and get the smoothed curve in the plots. One is obtained by using hybrid control strategy and another is obtained by using traditional fuzzy controller without bang-bang controller. Although these two curves both track the reference well with very good amplitude match (less than 5% error) and a few milliseconds misalignment in the time profile, by comparing these two curves, it can be found that the adjust time of the curve with hybrid control strategy is less than 0.03 s, which is much less than 0.05 s of other with traditional fuzzy controller. It proves effect of the hybrid control strategy.

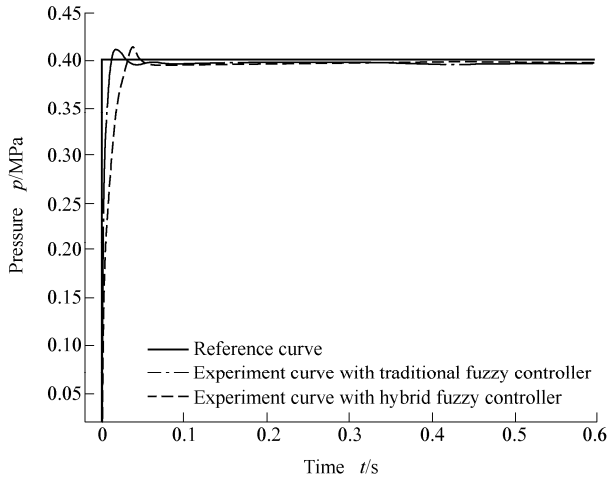

Fig. 11. Experimental results with a step signal

Fig. 12 shows the results of tracking a sinusoidal commander. This experiment is implemented to test the dynamic nature of the system. Although there is a little error and delay between the reference curve and the experiment curve, the system has good performance. According to the experiments, the system with the help of hybrid fuzzy control strategy can track an up to 5 Hz frequency sinusoidal command well.

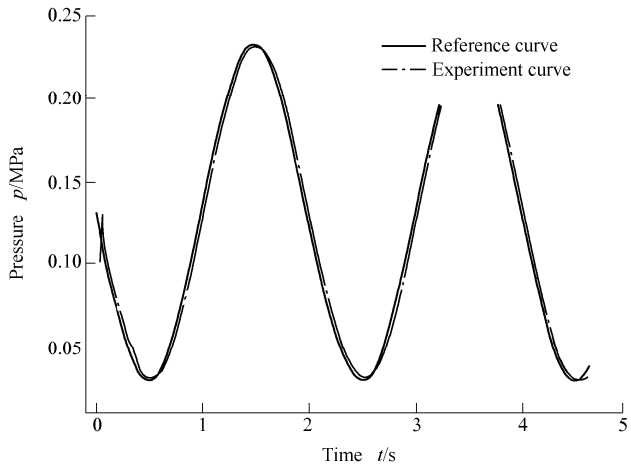

Fig. 12. Experiment results for sinusoidal pressure commands

After then, another two experiments are carried out to realize the bilateral teleoperation with simple motion, in which the slave manipulator is controlled for the shoulder abduction/ adduction (the movement of a bone away/toward the midline in the frontal plane) and extension/flexion of elbow (the movement in the sagittal plane) by the teleoperation with ZJUESA.

In the first experiment, the operator performs the shoulder abduction/adduction movement with ZJUESA, when the slave robot follows and holds up the load. With the force feedback on ZJUESA, the operator has feeling as if he holds the load directly without the mechanical structure, as shown in Fig. 13. Plots in Figs. 14, 15 show the torque and force on each joint on ZJUESA during the shoulder abduction/adduction movement from 45° to 90°(in the frontal plane) with 5 kg load. There are some remarks. In plots of Fig. 14 shoulder 3RPS-*x* means the torque around *x*-axis of 3RPS mechanism at shoulder and the same to shoulder 3RPS-*y*. Shoulder ring, elbow, wrist ring and wrist represent the torques on these joints, respectively. The characters shoulder 3RPS-1, shoulder 3RPS-2 and shoulder 3RPS-3 in Fig. 15 represent corresponding force on the cylinders on 3RPS parallel mechanism (referring to Fig. 3) with length L_1, L_2 and L_3, respectively.

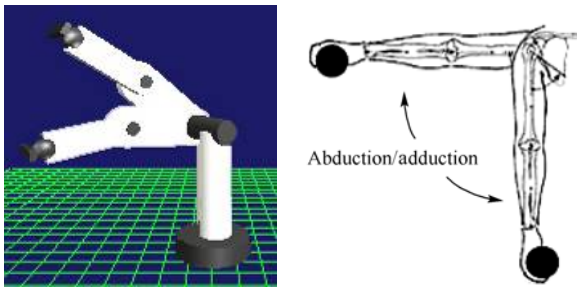

Fig. 13. Shoulder abduction/adduction teleoperation

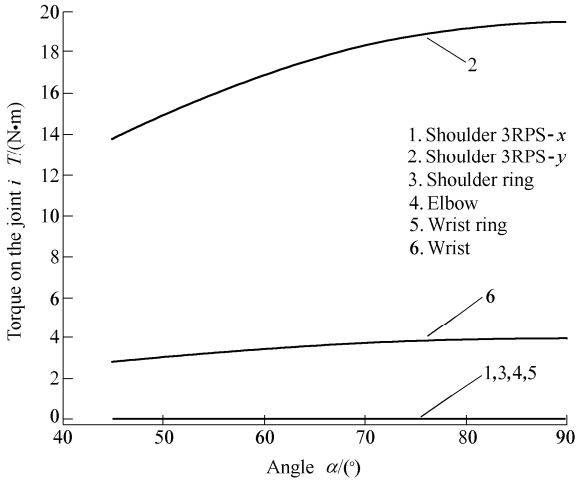

Fig. 14. Torques on the joints of the shoulder abduction/adduction for 5 kg load lifting

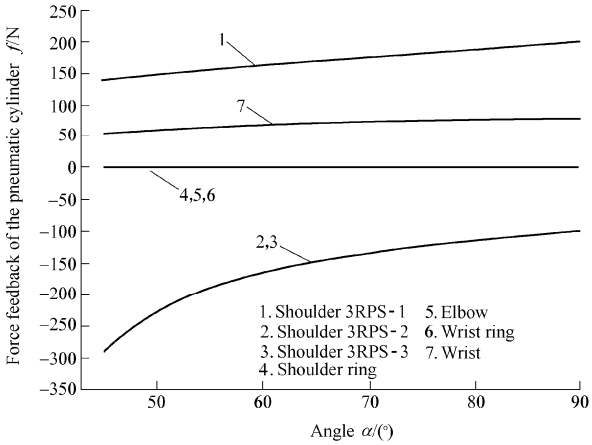

Fig. 15. Force feedback on the cylinders of the shoulder abduction/adduction for 5 kg load lifting

The operator teleoperates the slave manipulator with force feedback as if he performs for lifting a dumbbell or raising package in daily life (Fig. 16). Fig. 17 shows the moment on each joint during the process for producing the feeling of lifting a 10 kg dumbbell. Fig.18 depicts the force output of every pneumatic cylinder on ZJUESA.

All these results of experiments demonstrate the effect of ZJUESA system. ZJUESA performs well by following the motions of human upper-limb with little constrain and the pneumatic force feedback system supplies a proper force feedback tracking the reference well.

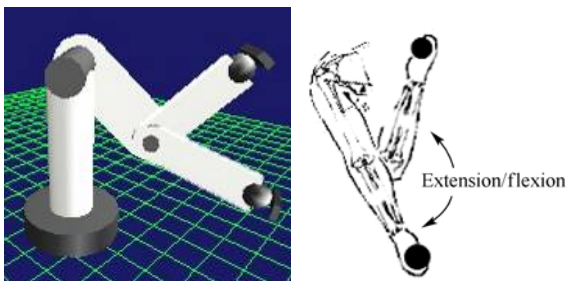

Fig. 16. Extension/flexion for elbow teleoperation

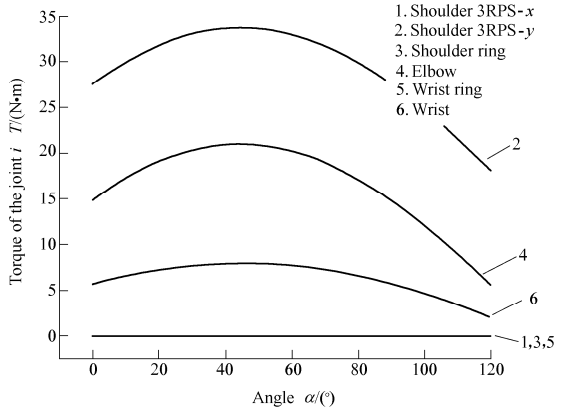

Fig. 17. Torques on the joints of the elbow extension/flexion for 10 kg load lifting

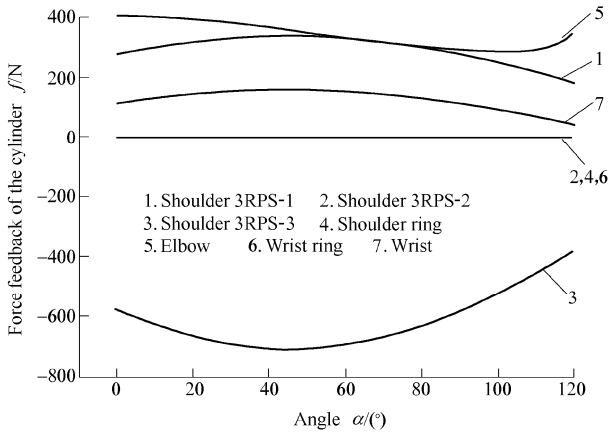

Fig. 18 Force feedback on the pneumatic cylinders of the elbow extension/flexion for 10 kg load lifting

6 Conclusions

(1) According to the anatomy of human upper-limb, the structure of ZJUESA is presented, which has 6 DOFs totally. 3RPS parallel mechanism analogy to the motion of muscle and ligament of human joint is employed to realize the shoulder structure with 3 degrees of freedom.

(2) The orthogonal experiment design method is employed for the optimal design. As a result a larger workspace of ZJUESA is obtained.

(3) In the interest of much more intuitive feelings in master-slave control process, the force feedback is realized simultaneously on ZJUESA by the pneumatic cylinders. And a novel hybrid fuzzy-controller is introduced in the Mega8 MCU as a unit of the distributed control system due to the non-linearity of the pneumatic system. The bang-bang control is utilized to drive the response of the system much more quickly and the fuzzy controller is activated when the output is near the set point, which needs accurate control.

(4) With sets of experiments, step, slope and sinusoidal commands are taken and the system shows a good performance, and a good agreement is found between the reference curves and experimental curves as well.

(5) The experiments of shoulder abduction/adduction and elbow extension/flexion teleoperation with force feedback are implemented. The results verify the feasibility of ZJUESA master-slave control system and the effect of the hybrid fuzzy-[illegible]e pneu

Font Size 10 p

Text Font Size 8 p, Line Spacing exactly 11 p

References

[1] SHERIDAN T B. *Automation, and human supervisory control-telerobotics*[M]. Cambridge MA: The MIT Press, 1992.

[2] GOERTZ R C, THOMPSON R C. Electronically controlled manipulators[J]. *Nucleonics*, 1954, 12(11): 46–47.

[3] DUBEY R, EVERETT S. Human-machine cooperative telerobotics using uncertain sensor and model data[C]//*International Conference on Robotics and Automation*, Lueven, Belgium, May 16–20, 1998: 1 615–1 622.

[4] SCHIELE A, VISENTIN G. The ESA human arm exoskeleton for space robotics telepresence[C]//*7th International Symposium on Artificial Intelligence, Robotics and Automation in Space*, Nara, Japan, May 19–23, 2003: 21–25.

[5] ROSEN J, HANNAFORD B, BURNS S. Neural control of an upper limb powered exoskeleton system-grant report[C]// *First NSF Robotics and Computer Vision (RCV) Workshop*, Las Vegas, USA, 2003: 26–27.

[6] ROSEN J, BRAND M, FUCHS M B, et al. A myosignal-based powered exoskeleton system[J]. *IEEE Transaction on Systems, Man., and Cybernetics-Part A: Systems and Humans*, 2001, 31(3): 210–222.

[7] BHARADWAJ K, HOLLANDER K W, MATHIS C A, et al. Spring over muscle (SOM) actuator for rehabilitation devices[C]//*Proceedings of the 26th Annual International Conference of the IEEE EMBS*, San Francisco, USA, September 1–5, 2004: 2 726–2 729.

[8] KOBAYASHI H, ISHIDA Y, SUZUKI H. Realization of all motion for the upper limb by a muscle suit[C]//*Proceedings of the IEEE International Workshop on Robot and Human Interactive Communication*, Okayama, Japan, September 20–22, 2004: 631–636.

[9] COHENA Y B, MAVROIDIS C, BOUZIT M, et al. Virtual reality robotic telesurgery simulations using MEMICA haptic system[C]// *Proceedings of SPIE's 8th Annual International Symposium on Smart Structures and Materials*, Newport, USA, March 5–8, 2001: 1–8.

[10] NAKAI A, OHASHI T, HASHIMOTO H. 7 DOF arm type haptic interface for teleoperation and virtual reality system[C]// *Proceedings of the IEEE/RSJ International Conference on Intelligent Robots and Systems*, Victoria, Canada, October, 1998: 1 266–1 231.

[11] KIM I, CHANG S, KIM J, et al. KIST hybrid master arm[C]// *Proceedings of the ASME Dynamic Systems and Control Division*, Nashville, USA, November 14–19, 1999: 195–204.

[12] JEONG Y, LEE D, KIM K, et al. A wearable robotics arm with high force-reflection capability[C]//*Proceedings of the IEEE International Workshop on Robot and Human Interactive Communication*, Osaka, Japan, September 27–29, 2000: 27–29.

[13] The triplex design group of Chinese Association of Statistics. *Orthogonal method and triplex design*[M]. Beijing: Science Press, 1987. (in Chinese)

[14] KIM Y S, LEE J, LEE S, et al. A force reflected exoskeleton-type masterarm for human-robot interaction[J]. *IEEE Transactions on Systems, Man. and Cybernetics-Part A: Systems and Humans*, 2005, 35(2): 198–212.

[15] LAWRENCE D A. Designing teleoperator architectures for

transparency[C]// *IEEE Int. Conf. on Robotics and Automation*, Nice, France, May, 1992: 1 406–1 411.
[16] RAJU G J. Design issues in 2-port network models of bilateral remote manipulation[C]// *Proceedings of the IEEE International Conference on Robotics and Automation*, Piscataway, NJ, USA, May 14–19, 1989: 1 313–1 321.
[17] YOKOKOHJI Y, YOSHIKAWA T. Bilateral control of master-slave manipulators for ideal kinesthetic coupling-formulation and experiment[J]. *IEEE Transactions on Robotics and Automation*, 1994, 10(5): 605–620.
[18] TORTORA G J, GRABOWSKI S R. *Introduction to the human body-the essentials of anatomy and physiology*[M]. 5th edition. New York: John Wiley & Sons, Inc., 2001.
[19] LENARCIC J, STANISIC M. A humanoid shoulder complex and the humeral pointing kinematics[J]. *IEEE Transaction on Robotics and Automation*, 2003, 19(3): 499–506.
[20] VEEGER H E J. The position of the rotation center of the glenohumeral joint[J]. *Journal of Biomechanics*, 2000, 12: 1 711–1 715.
[21] FANG K T, MA C X. *Orthogonal and uniform experimental design* [M]. Beijing: Scienc[illegible] 2000. (in Chinese)
[22] AMAGO T. Sizing [illegible] using response surface method in FOA[J]. R&D [illegible]
[23] Shanghai Scie[illegible] *of the orthogonal experiment design-multi factors experiment method*[M]. Shanghai: Shanghai People's Press, 1975. (in Chinese)
[24] YANG C J, NIU B, ZHANG J F, et al. Different structure based control system of the puma manipulator with an arm exoskeleton[C]// *Proceedings of the IEEE Conference on Robotics, Automation and Mechatronics*, Singapore, December 12–15, 2004: 572–577.
[25] KAITWANIDVILAI S, PARNICHKUN M. Force control in a pneumatic system using hybrid adaptive neuro-fuzzy model reference control[J]. *Mechatroincs*, 2005, 15(1): 23–41.
[26] AHN K, YOKOTA S. Intelligent switching control of pneumatic actuator using on/off solenoid valves[J]. *Mechatroincs*, 2005, 15(6): 683–702.
[27] SHIH M C, MA M A. Position control of a pneumatic cylinder using fuzzy PWM control method[J]. *Mechatronics*, 1998, 8(3): 241–253.
[28] MESSINA A, GIANNOCCARO N I, GENTILE A. Experimenting and modelling the dynamics of pneumatic actuators controlled by the pulse width modulation (PWM) technique[J]. *Mechatroincs*, 2005, 15(7): 859–881.
[29] XU W L, WU R H. Lyapunov's indirect method for stability analysis of fuzzy control system[J]. *Journal of Hunan University (Natural Sciences)*, 1998, 31(3): 86–89. (in Chinese)
[30] JENKINS D, PASSINO K M. An introduction to nonlinear analysis of fuzzy control systems[J]. *Journal of Intelligent and Fuzzy Systems*, 1999, 7(1): 75–103.
[31] BARTH E J, ZHANG J L, GOLDFARB M. Control design for relative stability in a PWM-controlled pneumatic system[J]. *Journal of Dynamic Systems, Measurement, and Control*, 2003, 125(9): 504–508.
[32] ZHANG J F, YANG C J, CHEN Y. *Use orthogonal experimental method to the optimal design for exoskeleton arm*[J]. WEASA Transactions on Systems, 2007, 6(6): 1 095–1 101.
[33] CHEN Y, ZHANG J F, YANG C J, et al. Design and hybrid control of the pneumatic force-feedback systems for arm-exoskeleton by using on/off valve[J]. *Mechantronics*, 2007, 17(7): 325–335.
[34] CHEN Y, ZHANG J F, YANG C J, et al. The workspace mapping with deficient DOF space for the puma 560 robot and its exoskeleton-arm by using orthogonal experiment design method[J]. *Robotics and Computer Integrated Manufacturing*, 2006, 23(4): 478–487.
[35] HUA[illegible] *and control theory of the parallel robot*[M][illegible] Machine Press, 1997. (in Chinese)

Font Size 10 p

Give his full name for a Chinese author. Avoid using an abbreviation.

Text Font Size 9 p, Line Spacing exactly 11 p; Leave one blank line after a paragraph.

Biographical notes

ZHANG Jiafan, born in 19[illegible] *State Key Laboratory of Flu[illegible] Zhejiang University, China.* [illegible] *Shanghai Jiaotong University,* [illegible] in 2003. His research interests include man-machine system and intelligent robotics.
Tel: +86-571-87953096; E-mail: caffeezhang@hotmail.com

FU Hailun, born in 1977, is currently an engineer at *Zhejiang Province Institute of Metrology, China*. He received his master degree on mechatronidcs in *Zhejiang University, China*, in 2006.

DONG Yiming, born in 1983, is currently a master candidate at *State Key Laboratory of Fluid Power Transmission and Control, Zhejiang University, China*.
E-mail: tim830528@163.com

ZHANG Yu, born in 1985, is currently a master candidate at *State Key Laboratory of Fluid Power Transmission and Control, Zhejiang University, China*.
E-mail: zhangyu_mm@hotmail.com

YANG Canjun, born in 1969, is currently an professor at *Zhejiang University, China*. He received his PhD degree from *Zhejiang Universtiy, China*, in 1997. His research interests include mechachonics engineering, man-machine system, robotics and ocean engineering.
Tel: +86-571-87953759; E-mail: ycj@sfp.zju.edu.cn

HEN Ying, born in 1962, is currently a professor and a PhD candidate supervisor at *State Key Laboratory of Fluid Power Transmission and Control, Zhejiang University, China*. His main research interests include mechachonics engineering, fluid power transmission and control, ocean engineering.
E-mail: ych[illegible]

Font Size 12 p

Appendix

Text Font Size 10 p

Appendix and supplement both mean[illegible]terial added at the end of a book. An appendix gives useful additional information, but even without it the rest of the book is complete: In the appendix are forty detailed charts. A supplement, bound in the book or published separately, is given for comparison, as an enhancement, to provide corrections, to present later information, and the like: A yearly supplement is issue.